An Efficient Current-Voltage Model for the AlGaAs/GaAs N-p Heterojunction Diode and its Application to HBTs

Jae-Hong Choi and Kae-Dal Kwack

Abstract

The new classified model for N-p heterojunction diode is derived and used extensively in analyzing the current-voltage(I-V) characteristics of the HBTs. A new classification method is presented in order to simplify I-V equations and easily applied to the modeling of HBTs. This classification method is characterized by the properties of devices such as the high level injection, the thickness of one or both bulk regions, the surface recombination and the generation-recombination. The simulation results using the proposed model agree well with the experimentally observed I-V behaviors and show good efficiencies in its application to HBTs with respect to mathematical formulation.

I. Introduction

HBT with a wide bandgap emitter has advantages compared with the conventional homojunction transistor in many respects. The AlGaAs / GaAs heterojunction devices are attractive for the high speed digital circuit applications which require the performance such as a high voltage, a high current density, a high power and a considerable high efficiency in recent years[1-3]. In comparison with other conventional transistors, the ones using heterojunctions become increasingly important in semiconductor devices and have already found applications in excellent millimeter and micro-wave devices with high cutoff and oscillation frequencies[4]. With the rapid advances of heterojunction devices, it is necessary to have a simple and accurate device model to analyze the heterojunction circuits and devices. Theoretical analyses for heterojunction devices have been reported by some authors using various modeling techniques such as one and two dimensional numerical methods[5-6], Monte-Carlo technique[7], and complicated analytic models[8-10].

Lundstrom and Taeyong Won proposed that the carrier flow across the heterojunction interface could be modeled by the generalized interface transport velocity S[11-12] ; using such a velocity, they derived an Ebers-Moll-like model that would be valid for abrupt or graded, and single or double HBTs. Ryum and Abdel-Motaleb derived a Gummel-Poon-like model[13] which was strictly valid only for a low level injection. A self-consistent two dimensional model was also developed by Marty *et al.*[14] to investigate the electrothermal problem in AlGaAs / GaAs HBT. Although early works on heterojunctions identified an important I-V mechanism, but the modeling procedures was time-consuming and sophisticated to get the characteristic equations of the AlGaAs / GaAs N-p and HBT models. For these reasons, it is difficult to apply such models for the circuit and the device design of heterojunction. Therefore, the generalized modeling technique is necessary for I-V characteristics of heterojunction. The purpose of this paper is to generalize and clarify the I-V model of HBT's using a modeling technique in N-p heterojunction. This model includes the various heterojunction material parameters and the effects such as high level injections, surface recombination effects, bulk size effects and generation-recombination currents by a simple classification.

II. Derivations of N-p Heterojunction Diode Model

1. Diffusion Current-Voltage Model

First of all, a simple structure of a N-p heterojunction is assumed. A typical energy band diagram for AlGaAs / GaAs material system is shown in Fig. 1, where x_{n1} and x_{p1} are the edges of the N-p space-charge-region(SCR) and x_{n2}, x_{p2} are the edges of N, p region, respectively. The other symbols of this figure are conventional notations. The equation of state for bulk p-GaAs region is reduced to the following minority carrier equation.

$$D_n \frac{d^2 \delta n(x)}{dx^2} - \frac{\delta n(x)}{\tau_n} = 0 \tag{1}$$

Manuscript received April 1, 1997; accepted July 14, 1997.

J. H. Choi and K. D. Kwack are with Department of Electronic Engineering, Hanyang University, Korea.

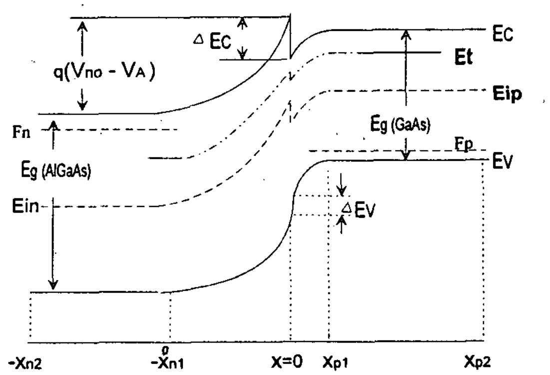

Fig. 1. Energy band structure of AlGaAs / GaAs N-p heterojunction.

Where $\delta n(x)$ is the excess carrier density, τ_n is the the life time of electron. The boundary conditions at $x=x_{p1}$ and $x=x_{p2}$ can be expressed as following in terms of high level injection term H_n [15] and surface recombination velocity s_p, which are directly related to the heterojunction material parameters.

$$\delta n(x=x_{p1})=\delta n(x_{p1})=n_{po}(e^{\frac{qV}{kT}}-1)H_n \tag{2.a}$$

$$J_n(x=x_{p2})=qD_n\frac{d\delta n(x)}{dx}=-q s_p \delta n(x_{p2}) \tag{2.b}$$

Therefore, the electron excess carrier density $\delta n(x)$ in p-GaAs region is

$$\delta n(x)=\delta n(x_{p1})\left\{\frac{\cosh(\frac{x-x_{p2}}{L_n})-\frac{L_n s_p}{D_n}\sinh(\frac{x-x_{p2}}{L_n})}{\cosh(\frac{x_{p2}-x_{p1}}{L_n})+\frac{L_n s_p}{D_n}\sinh(\frac{x_{p2}-x_{p1}}{L_n})}\right\}, \tag{3}$$

$$x_{p1}\le x\le x_{p2}$$

The electron current density $J_n(x)$ in the neutral p type region can be derived by applying the current density equation for electron.

$$J_n(x)=q(\frac{D_n}{L_n})\,\delta n(x_{p1})\left\{\frac{\sinh(\frac{x-x_{p2}}{L_n})-\frac{L_n s_p}{D_n}\cosh(\frac{x-x_{p2}}{L_n})}{\cosh(\frac{W_p}{L_n})+\frac{L_n s_p}{D_n}\sinh(\frac{W_p}{L_n})}\right\} \tag{4}$$

Where, W_p is the bulk layer thickness of p-GaAs region, L_n is the diffusion length which equals to $\sqrt{D_n\tau_n}$, D_n is diffusion coefficient.

Substitution of $x=x_{p1}$ for eqn. (4) results in a simply clarified expression as shown in eqn. (5).

$$J_n(x_{p1})=-q(\frac{D_n}{L_n})n_{po}H_n S_N B_n(e^{\frac{qV}{kT}}-1) \tag{5}$$

where S_N and B_n can be defined as following

$$S_N\equiv\frac{\tanh^2(\frac{W_p}{L_n})+\frac{L_n s_p}{D_n}\tanh(\frac{W_p}{L_n})}{1+\frac{L_n s_p}{D_n}\tanh(\frac{W_p}{L_n})} \tag{6}$$

$$B_n\equiv\cosh(\frac{W_p}{L_n})\,/\,\sinh(\frac{W_p}{L_n})=\coth(\frac{W_p}{L_n}) \tag{7}$$

Following the same procedure as used in obtaining eqn. (5), the hole excess carrier density $\delta p(x)$ in n-AlGaAs is

$$\delta p(x)=\delta p(-x_{n1})\left\{\frac{\cosh(\frac{x_{n2}+x}{L_p})-\frac{L_p s_n}{D_p}\sinh(\frac{x_{n2}+x}{L_p})}{\cosh(\frac{x_{n2}-x_{n1}}{L_p})-\frac{L_p s_n}{D_p}\sinh(\frac{x_{n2}-x_{n1}}{L_p})}\right\}, \tag{8}$$

$$-x_{n2}\le x\le -x_{n1}$$

The boundary conditions of n side surface $x=-x_{n2}$ in Fig. 1 can be treated in the same way. Therefore, the hole current density $J_p(x)$ can be obtained as eqn. (9).

$$J_p(x)=-q(\frac{D_p}{L_p})\,\delta p(-x_{n1})\left\{\frac{\sinh(\frac{x_{n2}+x}{L_p})-\frac{L_p s_n}{D_p}\cosh(\frac{x_{n2}+x}{L_p})}{\cosh(\frac{W_n}{L_p})-\frac{L_p s_n}{D_p}\sinh(\frac{W_n}{L_p})}\right\} \tag{9}$$

Where, W_n is the thickness of n-AlGaAs bulk region, the diffusion length L_p is expressed as a function of diffusivity D_p, life time of hole τ_p. Substitution of $x=-x_{n1}$ for eqn. (9) results in eqn. (10).

$$J_p(-x_{n1})=-q(\frac{D_p}{L_p})p_{no}H_p S_P B_p(e^{\frac{qV}{kT}}-1) \tag{10}$$

Where, H_p is the high level injection term, which consists of heterojunction material parameters [15]. Also, the S_P and B_p can be expressed in terms of surface recombination and bulk size factors in n-AlGaAs side as eqn. (11) and eqn. (12).

$$S_P\equiv\frac{\tanh^2(\frac{W_n}{L_p})+\frac{L_p s_n}{D_p}\tanh(\frac{W_n}{L_p})}{1+\frac{L_p s_n}{D_p}\tanh(\frac{W_n}{L_p})} \tag{11}$$

$$B_p\equiv\cosh(\frac{W_n}{L_p})\,/\,\sinh(\frac{W_n}{L_p})=\coth(\frac{W_n}{L_p}) \tag{12}$$

Hence, we finally obtain the generalized and clarified expression for N-p total current density by adding eqn. (5) and eqn. (10).

$$J_{tot}=-q\left\{(\frac{D_n}{L_n})n_{po}H_n S_N B_n+(\frac{D_p}{L_p})p_{no}H_p S_P B_p\right\}\left(e^{\frac{qV}{kT}}-1\right) \tag{13}$$

The total diffusion current is classified by the characterized factors (H, S, E) which involve the heterojunction parameters, surface recombination velocities and bulk layer thicknesses and high level injections. The eqn. (13) is applied for general cases. But for high level injection, the parameters of H_n and H_p in eqn. (13) are set to unity. And the bulk size effects B_n and B_p are the same method as the case of H_n and H_p. Also, for large area metallic ohmic contacts used as terminals (i. e., its surface recombination velocities s_n, s_p are very high), the defined function S_N or S_P reduces to unity. To be sure, substituting the physical parameters for heterojunction to those for homojunction, eqn. (13) result in the conventional I-V equation of homojunction bipolar transistors. Therefore, the resulting equation is generally applicable and very simple mathematical expression in that the characteristics of the derived equation are described in detail according to various device conditions.

2. *Generation-Recombination Current-Voltage Model in N-p SCR*

From the viewpoint of generation-recombination mechanism in N-p SCR, we previously reported the result [18]. The recombination process was assumed to be the Shockley-Read-Hall type through a single recombination center. The generation-recombination I-V model for heterojunction was presented in consideration of the trap density and level in AlGaAs / GaAs compound semiconductor within the SCR. The presented model differs from the previous model [15, 19] with respect to the assumption of the important factors(τ_n, τ_p, E_t, E_i). Therefore, these characteristic models comprise not only the previous models, but also give satisfactory results in many aspects. The resulting equations are as follows.

$$J_{SRH(n)} = -\frac{4\varepsilon_n kT}{qN_d x_{n1}}\, n_{in}\; T_n(b)\; \sinh\left(\frac{qV_A}{2kT}\right), \quad -x_{n1} \le x \le 0 \qquad \textbf{(14)}$$

$$J_{SRH(p)} = -\frac{4\varepsilon_p kT}{qN_a x_{p1}}\, n_{ip}\; T_p(b)\; \sinh\left(\frac{qV_A}{2kT}\right), \quad 0 \le x \le x_{p1} \qquad \textbf{(15)}$$

III. Application to N-p-n HBT

1. *Basic Current Components*

Based on the proposed model in section II, the I-V characteristics of AlGaAs / GaAs HBT's with various effects will be analyzed, especially focused on the generalized and clarified equation. Fig. 2 illustrates the simplest HBT structure consisting of a wide-bandgap AlGaAs emitter(n-type), a heavily doped GaAs base(p-type), a lightly doped GaAs collector(n-type), and the energy band diagram under a forward-active operation (base-emitter voltage $V_{BE} > 0$ and collector-base voltage $V_{CB} < 0$). The current densities between N-emitter and p-base are obtained by adding diffused current density for electron and hole.

The boundary conditions in the base are

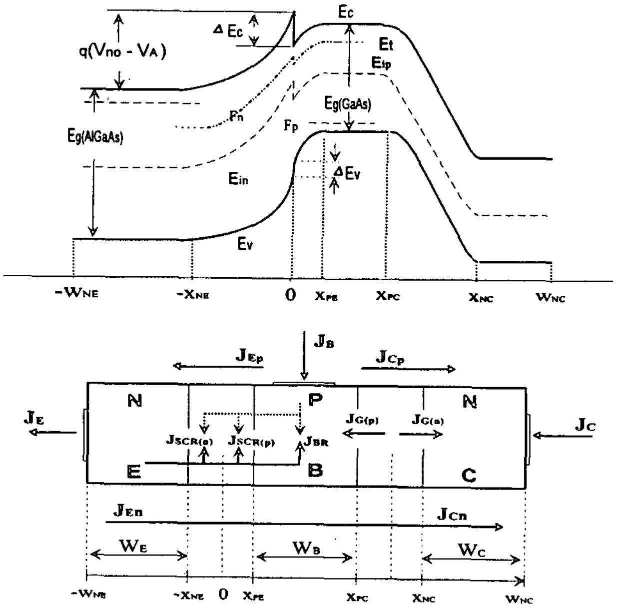

Fig. 2. N-p-n AlGaAs/GaAs/GaAs heterojunction bipolar transistor energy band diagram and current components.

$$\delta n(x = x_{pE}) = \delta n_B(x_{pE}) = n_B\left(e^{\frac{qV_{BE}}{kT}} - 1\right) H_{nE} \qquad \textbf{(16.a)}$$

$$\delta n(x = x_{pC}) = \delta n_B(x_{pC}) = n_B\left(e^{\frac{qV_{BC}}{kT}} - 1\right) H_{nC} \qquad \textbf{(16.b)}$$

where,

$$H_{nE} \equiv \frac{1 + \dfrac{p_{Eo}}{n_{Eo}}\, e^{\frac{qV_{BE}}{kT}}}{1 - e^{\frac{2q(V_{BE} - V_{noE}) - \Delta E_{gE}}{kT}}} \qquad \textbf{(17.a)}$$

and,

$$H_{nC} \equiv \frac{1 + \dfrac{p_{Co}}{n_{Co}}\, e^{\frac{qV_{BC}}{kT}}}{1 - e^{\frac{2q(V_{BC} - V_{noC}) - \Delta E_{gC}}{kT}}} \qquad \textbf{(17.b)}$$

The eqns. (17) contain the potential V_{noE} and energy difference ΔE_{gE} in base-emitter, the potential V_{noC} and energy difference ΔE_{gC} in the base-collector. Applying the electron excess carrier density $\delta n_B(x)$ in the base to current density equation of electron, the emitter current density for electron becomes eqn. (18)

$$J_{EN}(x_{pE}) = -q\left(\frac{D_B}{L_B}\right) n_{Bo}\left\{H_{nE} B_B\left(e^{\frac{qV_{BE}}{kT}} - 1\right) - H_{nC} B_{BC}\left(e^{\frac{qV_{BC}}{kT}} - 1\right)\right\} \textbf{(18)}$$

where B_B and B_{BC} are expressed as $\coth(\frac{W_B}{L_B})$ and $\operatorname{csc}h(\frac{W_B}{L_B})$, respectively. Using the same way from eqn. (8) eqn. (10), the hole current density in N-emitter side is

$$J_{EP}(-x_{nE}) = -q\left(\frac{D_E}{L_E}\right) p_{Eo} H_{pE} S_E B_E \left(e^{\frac{qV_{BE}}{kT}} - 1\right) \qquad \textbf{(19)}$$

where H_{pE}, S_E and B_E are

$$H_{pE} \equiv \frac{1+\frac{n_{Bo}}{p_{Bo}}\, e^{\frac{qV_{BE}}{kT}}}{1-e^{\frac{2q(V_{BE}-V_{noE})-\Delta E_{gE}}{kT}}} \tag{20}$$

$$S_E \equiv \frac{\tanh^2(\frac{W_E}{L_E})+\frac{L_E s_{nE}}{D_E}\tanh(\frac{W_E}{L_E})}{1+\frac{L_E s_{nE}}{D_E}\tanh(\frac{W_E}{L_E})} \tag{21}$$

$$B_E \equiv \cosh(\frac{W_E}{L_E}) / \sinh(\frac{W_E}{L_E}) = \coth(\frac{W_E}{L_E}) \tag{22}$$

The current components between p-base and n-collector are obtained by combining the electron current density J_{CN} and the hole J_{CP}. A junction between the base and collector which is the combination of two different materials results in the double heterojunction bipolar transistor(D-HBT). Substituting the same-materials for the hetero-materials in this region results in the single heterojunction bipolar transistor(S-HBT). In the same way, the collector current densities are

$$J_{CN}(x_{pC}) = q(\frac{D_B}{L_B})\, n_{Bo}\left\{ H_{nC} B_B (e^{\frac{qV_{BC}}{kT}}-1) - H_{nE} B_{BC} (e^{\frac{qV_{BE}}{kT}}-1)\right\} \tag{23}$$

$$J_{CP}(x_{nC}) = q(\frac{D_C}{L_C})\, p_{Co} H_{pC} S_C B_C (e^{\frac{qV_{BC}}{kT}}-1) \tag{24}$$

where,

$$H_{pC} \equiv \frac{1+\frac{n_B}{p_B}\, e^{\frac{qV_{BC}}{kT}}}{1-e^{\frac{2q(V_{BC}-V_{noC})-\Delta E_{gC}}{kT}}} \tag{25}$$

and

$$S_C \equiv \frac{\tanh^2(\frac{W_C}{L_C})+\frac{L_C s_{nC}}{D_C}\tanh(\frac{W_C}{L_C})}{1+\frac{L_C s_{nC}}{D_C}\tanh(\frac{W_C}{L_C})} \tag{26}$$

$$B_C \equiv \cosh(\frac{W_C}{L_C}) / \sinh(\frac{W_C}{L_C}) = \coth(\frac{W_C}{L_C}) \tag{27}$$

2. Generation-Recombination and Base Recombination Current Components

The major sources of generation-recombination effects in device are the emitter-base and the base-collector depletions. The generation current density at base-collector SCR and the recombination current density at emitter-base SCR are obtained in active region, respectively. Using the eqn. (14) and (15) on each side, the recombination and the generation current density equations are modified to

$$J_{SRH(V_{BE}>0)} = -\frac{4kT}{q}\left[\frac{\varepsilon_E n_{iE}}{N_E x_{nE}} T_E(b) + \frac{\varepsilon_B n_{iB}}{N_B x_{pE}} T_B(b)\right]\sinh\left(\frac{qV_{BE}}{2kT}\right) \tag{28}$$

$$J_{SRH(V_{BC}<0)} = -\frac{4kT}{q}\left[\frac{\varepsilon_C n_{iC}}{N_C x_{nC}} T_C(b) + \frac{\varepsilon_B n_{iB}}{N_B x_{pC}} T_B(b)\right]\sinh\left(\frac{qV_{BC}}{2kT}\right) \tag{29}$$

where n_i, ε and N are the intrinsic carrier densities, the dielectric constants and the doping densities on each side, respectively. The characteristic function $T(b)$ is a function of many parameters involving a trap related of heterojunction [18].

On the other hand, the base recombination current density is obtained by integrating the excess carrier density of electron $\delta n_B(x)$ in a p-base bulk region.

Therefore, the base recombination current density is defined as

$$J_{BR} = -\frac{q}{\tau_B}\int_{x_{pE}}^{x_{pC}} \delta n_B(x)\, dx \tag{30}$$

Integrating eqn. (30) yields

$$J_{BR} = -q(\frac{L_B}{\tau_B})\, n_{Bo}(B_B-B_{BC})\left\{ H_{nE}(e^{\frac{qV_{BE}}{kT}}-1) + H_{nC}(e^{\frac{qV_{BC}}{kT}}-1)\right\} \tag{31}$$

Usually, for most practical heterojunction bipolar transistors, the base width W_B is very smaller than L_B. The term of $B_B - B_{BC}$ in eqn. (31) as a function of base width can be further simplified as $\frac{W_B}{2L_B}$. Under a uniform base distribution, the base transit time τ_B is being $\frac{W_B^2}{2D_B}$, eqn. (31) becomes

$$J_{BR} = -q(\frac{D_B}{W_B})\, n_{Bo}\left\{ H_{nE}(e^{\frac{qV_{BE}}{kT}}-1) + H_{nC}(e^{\frac{qV_{BC}}{kT}}-1)\right\} \tag{32}$$

3. Terminal Current Density

In the previous sections, we obtain the generalized and clarified current density equations for HBT by applying the results of N-p heterojunction diode current density equations under normal operation.

In conclusion, the emitter, the collector, and the base terminal current densities can be rewritten in the following equations

$$\begin{aligned} J_E &= J_{EN}+J_{EP}+J_{SRH(V_{BE}>0)} \\ &= -q\left[\left\{(\frac{D_B}{L_B}) n_{Bo} H_{nE} B_B + (\frac{D_E}{L_E}) p_{Eo} H_{pE} S_E B_E\right\}(e^{\frac{qV_{BE}}{kT}}-1) \right. \\ &\quad \left. -(\frac{D_B}{L_B}) n_{Bo} H_{nC} B_{BC}(e^{\frac{qV_{BC}}{kT}}-1)\right] + J_{SRH(V_{EB}>0)} \end{aligned} \tag{33}$$

$$\begin{aligned} J_C &= J_{CN}+J_{CP}+J_{SRH(V_{BC}<0)} \\ &= -q\left[(\frac{D_B}{L_B}) n_{Bo} H_{nE} B_{BC}(e^{\frac{qV_{BE}}{kT}}-1) - \left\{(\frac{D_B}{L_B}) n_{Bo} H_{nC} B_B \right.\right. \\ &\quad \left.\left. + (\frac{D_C}{L_C}) p_{Co} H_{pC} S_C B_C\right\}(e^{\frac{qV_{BC}}{kT}}-1)\right] + J_{SRH(V_{BC}<0)} \end{aligned} \tag{34}$$

and,

$$\begin{aligned} J_B &= J_{BR}+J_{EP}-J_{CP}+(J_{SRH(V_{BE}>0)}-J_{SRH(V_{BC}<0)}) \\ &= -q\Bigg[\left\{(\frac{D_B}{W_B})n_{Bo}H_{nE}+(\frac{D_E}{L_E})p_{Eo}H_{pE}S_E B_E\right\}(e^{\frac{qV_{BE}}{kT}}-1) \\ &\quad +\left\{(\frac{D_B}{W_B})n_{Bo}H_{nC}+(\frac{D_C}{L_C})p_{Co}H_{pC}S_C B_C\right\}(e^{\frac{qV_{BC}}{kT}}-1)\Bigg] \\ &\quad +(J_{SRH(V_{BE}>0)}-J_{SRH(V_{BC}<0)}) \end{aligned} \tag{35}$$

Ⅳ. Results and Discussions

To show the validity of this model, we compare the simulated results with numerical [16] and experimental data [17] for two samples in the name of HBT-A and HBT-B. The results of this simulation for samples are plotted in Fig. 3 and Fig. 4.

For HBT-A, the material parameters for calculations are adopted from Refs. [16] and [20]. Fig. 3 shows the results of the collector current density J_C and the base current density J_B versus the base-emitter bias $V_{BE}(V)$ with V_{CE}=2.5 [V] in room temperature. Using this model, the simulated results of J_C and J_B are considerable agreement with the numerical data, especially in a range of the operational bias for transistor. However, there is a little deviation with numerical data in the range of the high base-emitter bias(about V_{BE}=1.4[V]), it is considered that the voltage drop was neglected for the respective bulk regions in the proposed model. Compare to the numerical methods, this model gives a easier procedure to get the results and its application for HBTs.

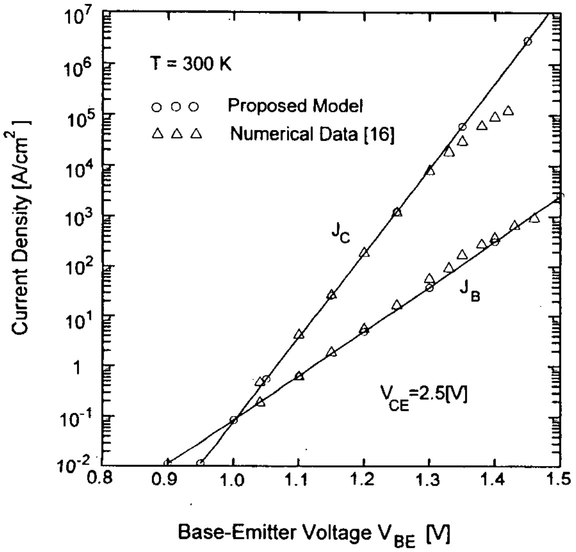

Fig. 3. The characteristics of the current densities(J_c, J_B) with V_{BE} for HBT-A.

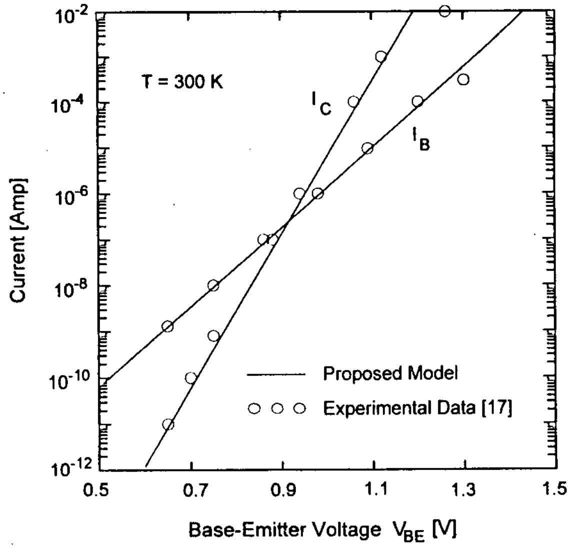

Fig. 4. The calculated currents(I_C, I_B) with V_{BE} for HBT-B.

A Gummel plot of the current I_B, I_C is shown in Fig. 4 with the experimental data [17] under the other conditions for varying the base-emitter bias V_{BE} [V]. In calculations we used the material parameters given by [17]. Comparing the results of presented model with those of experimental data in Fig. 4, the results coincide well with each other in the small forward bias considering the generation-recombination current-voltage mechanism and the normal operational bias considering the diffusion current-voltage mechanism. Therefore, agreements with both results in these regions are notable that the proposed model take well account of the generation-recombination and diffusion current-voltage mechanism. As can be seen in this results, a difference between two data in the latter part has occurred at a high bias (above $V_{BE}=1.2\,[V]$) because the bulk resistance effect and the temperature effect are not considered in the model. Nevertheless, the available results in this model do cover a useful bias range. Also, a thin part of the AlGaAs emitter near the p-n junction can be lightly doped and the base heavily doped(about $10^{19}cm^{-3}$), and the rest of the neutral emitter region can be heavily doped for smaller emitter bulk resistance. Such a doping configuration reduces the bulk resistance compared with the conventional homojunction transistor. As a result, it is possible that the bulk resistance effects can be neglected in order to simplify the I-V characteristic equation of a proposed model.

Using the data given in Fig. 4, the variations of d.c. current-gain is shown in Fig. 5, according to the collector current. This plot shows some difference the measured data and the previous data with calculated data. On the other hand, the result for the proposed model approaches the measured data and improves the current gain with respect to the previous data. From these facts, the proposed model is more accurate and efficient than the previous model.

Ⅴ. Conclusion

From the analysis of AlGaAs/GaAs N-p heterojunction diode, the I-V characteristic equation of HBT has been derived by the

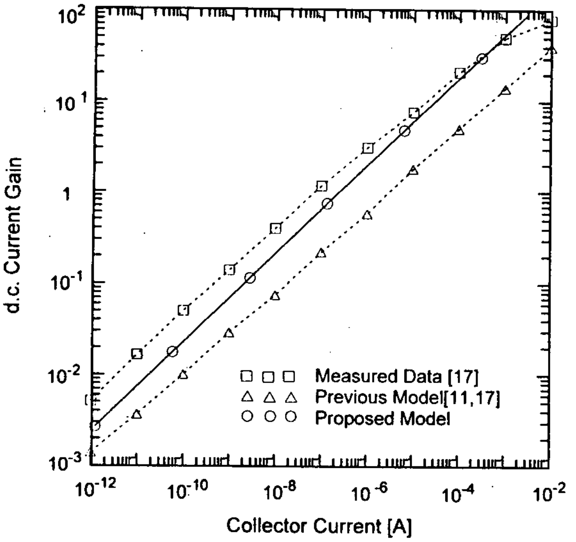

Fig. 5. The characteristics of d.c. current gain with collector current density.

clarified functions which include the properties for the high level injection(H), the thickness of bulk regions(B), the generation-recombination mechanism(T) and the surface recombination(S). It has been shown that the formulation presented in this paper is very simple for the mathematical expressions and easy to understand for the analysis of I-V characteristics, which has the advantage to apply for the various kinds of heterojunction devices. The analysis for AlGaAs/GaAs HBT has been mainly treated in this paper, but many concepts and modeling techniques presented are also applicable to other types of HBTs. The validity of the proposed model is illustrated by comparing the simualtion results with other published experimental and numerical results.

References

[1] H. Kroemer, "Heterojunction bipolar transistors and integrated circuits," *Proc. IEEE Trans. Electron Devices*, Vol. 70, p. 13, 1982.

[2] J. A. Higgins, "Heterojunction bipolar transistors for high efficiency amplifiers," *IEEE GaAs IC Symp., Tech. Dig.*, p. 33, 1988.

[3] P. M. Asbeck, M. F. Chang, J. A. Higgins, N. H. Sheng, G. J. Sullivan, and K. C. Wang, "GaAlAs/GaAs heterojunction bipolar transistors : Issues and prospects for application," *IEEE Trans. Electron devices*, Vol. 36, pp. 2032-2042, 1989.

[4] J. J. Liou, J. Jenkins, L. L. Liou, et al., "Bias, Frequency, and Area Dependencies of High frequency Noise in AlGaAs/GaAs HBT's," *IEEE Trans. Electron Devices*, Vol. 43, pp. 116-121, 1996.

[5] M. Kurata and J. Yoshida, "Modeling and characterization for high-speed GaAlAs-GaAs n-p-n heterojunction bipolar transistors," *IEEE Trans. Electron Devices*, Vol. 31, pp. 467-473, 1984.

[6] Y. S. Hiraoka, J. Yoshida, M. Azuma, "Two-Dimensional Analysis of Emitter-Size Effect on Current Gain for GaAlAs/GaAs HBT's," *IEEE Trans. Electron Devices*, Vol. 43, pp. 721-725, 1987.

[7] H. Nakajima, T. Ishibashi, "Monte Carlo Analysis of Nonequilibrium Electron Transport in InAlAs/InGaAs HBT's," *IEEE Electron Devices*, Vol. 40, pp. 1950-1956, 1993.

[8] S. Searles, D. L. Pulfrey, "An Analysis of Space-Charge-Region Recombination in HBT's," *IEEE Trans. Electron Devices*, Vol. 41, pp. 476-483, 1994.

[9] D. Parikh and Fredrik A. Lindholm, "A new Charge-Contral Model for Single- and Double-Heterojunction Bipolar Transistors," *IEEE Trans., Electron Devices*, Vol. 39, pp. 1303-1311, 1992.

[10] K. Park and K. Kwack, "A model for the current-voltage characteristics of MODFET's," *IEEE Trans. Electron Devices*, Vol. 33, pp. 676-679, 1986.

[11] M. S. Lundstrom, "An Ebers-Moll Model for the heterojunction Bipolar Transistor," *Solid-State Electronics*, Vol. 29, pp. 1173-1179, 1986.

[12] Taeyoung Won, "An investigation of Heterojunction Bipolar transistors By Molecular Beam Epitaxy," *ph.D. thesis*, University of Illinois at Urbana-Champaign, 1989.

[13] B. R. Ryum and I. M. Abedel-Motaleb, "A Gummel-Poon model for abrupt and graded heterojunction bipolar transistors," *Solid-State Electron.*, Vol. 33, p. 896, 1990.

[14] A. Marty, T. Camps, J. Tasselli, D. L. Pulfrey and J. P. Bailbe, "A self-consistent DC-AC two dimensional electro-thermal model for GaAlAs/GaAs microwave power HBT's," *IEEE Trans. Electron Devices*, Vol. 40, pp. 1202-1210, 1993.

[15] K. Park, J. Choi and K. Kwack, "An unified analytic model of N-p homo and heterojunctions for HBT applications," *J. of KITE*, Vol. 29-A, No. 6, pp. 6-13, 1992.

[16] L. L. Liou, C. I. Huang and J. Ebel, "Numerical studies of thermal effects on heterojunction bipolar transistor current-voltage characteristics using one-dimensional simulation," *Solid-State Electronics*, Vol. 35, pp. 579-585, 1992.

[17] M. E. Klausmeier-Brown, M. S. Lundstrom and M. R. Melloch, "The effects of heavy impurity doping on AlGaAs/GaAs bipolar transistors," *IEEE Trans. Electron Devices*, Vol. 36, pp. 2146-2155, 1989.

[18] J. Choi, H. Kim, *et al.*, "An efficient current-voltage model of SRH Generation-Recombination for $Al_xGa_{1-x}As$/GaAs N-p heterojunction devices," *International Semiconductor Device Research Symposium*, pp. 677-680, 1995.

[19] H. Ito, "Generation-Recombination current in the emitter-base junction of AlGaAs/GaAs HBTs," *Japanese J. Appl. Phys.*, Vol. 25, No. 9, pp. 1400-1404, 1986.

[20] S. Adachi, "GaAs,AlAs, and AlxGa1-xAs: Material parameters for use in research and device applications," *J. Appl. Phys.*, 58, 1985.

Jae-Hong Choi was born in Chungnam, Korea, in 1962. He received the B.S. and M.S. degrees in electronic engineering from Hanyang University in 1986 and 1989, respectively. He is currently in the course of Ph.D. at Hanyang University. His principal research interests include in device modeling, millimeter-wave semiconductor device modeling, and circuit design.

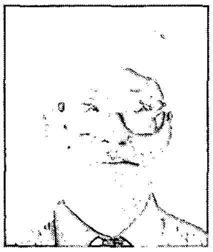

Kae-Dal Kwack (M'83) was born in Daegu, Korea, on February 13, 1950. He received the B.S. and M.S. degrees in electronic engineering from Hanyang University, Seoul, Korea, in 1974 and 1976, respectively, and the Ph.D. degrees in electronic engineering from the Institute National Polytechnique de Toulouse, E.N. S.E.E.H.T., Toulouse, France, in 1980. He is a Professor of Electronic Engineering at Hanyang University where he worked on the research of two-dimensional MOSFET simulation. He did research on Ⅲ-Ⅴ compound devices at Waseda University, Tokyo, and the University of California, Santa Barbara, in 1984 and 1985, respectively. Currently he is a professor of department of electronic engineering at Hanyang University. His research is currently focused on micro-wave semiconductor device modeling, and circuit design.